

π - d backbonding band dispersion and final-state effects for the $(2 \times 1) p2mg$ phase of CO on Ni(110)

H. Kuhlenbeck,* H. B. Saalfeld, U. Buskotte, and M. Neumann
*Fachbereich Physik, Universität Osnabrück, Barabarastrasse 7,
D-4500 Osnabrück, Federal Republic of Germany*

H.-J. Freund
*Lehrstuhl für Physikalische Chemie I, Ruhr-Universität Bochum,
D-4630 Bochum 1, Federal Republic of Germany*

E. W. Plummer
*Department of Physics, University of Pennsylvania,
Philadelphia, Pennsylvania 19104-6396*
(Received 3 October 1988)

Angle-resolved photoemission spectroscopy has been utilized to measure the dispersion and symmetry of the spectral features in the d -band region of Ni induced by the adsorption of CO. Very strong alterations of the d -band emission characteristics are observed when CO is adsorbed on Ni(110) in the $(2 \times 1) p2mg$ ordered phase. The high density and unique symmetry of this overlayer allow an unambiguous identification of the spectral features as the two-dimensional π - d surface bands induced by the chemical bond of CO to Ni, i.e., by the CO 2π -Ni $3d$ interaction.

INTRODUCTION

The adsorption of carbon monoxide onto a transition-metal surface has served as the test system in surface science for both new experimental techniques and theoretical approaches. In general, a fairly detailed picture of the bonding as well as a much better understanding of the capabilities of the measurement techniques has emerged from the numerous studies of CO adsorption systems. Surely this knowledge has been and will continue to be very useful in the study of other adsorption systems. Yet, there are still some unresolved questions about the adsorption of CO related to the picture of the bonding that has been developed from experiment and theory. One of these questions will be addressed in this paper, i.e., the nature of the occupied CO 2π -metal d bands formed when CO is adsorbed onto a metal surface. A preliminary account of this work has already been published.¹

It is necessary to briefly discuss the current picture of the bonding of CO to a transition-metal surface, so that the significance of this paper can be put into a proper perspective. Figure 1 shows a schematic diagram of the interaction of CO with a metal surface and the effect of the CO-CO interaction, which is always important at higher coverages. On the right-hand side the interaction of a CO molecule with a metal atom is depicted. The current understanding of the interaction can be simply described by considering the highest occupied orbital of free CO (5σ), the lowest unoccupied orbitals of free CO ($2\pi_x$ and $2\pi_y$), and the metal d bands. The CO interacts with the metal through these levels. The 5σ -metal interaction forms a bonding ($5\bar{\sigma}$) and an antibonding orbital ($5\sigma^*$), respectively, in Fig. 1. The bonding orbital is

obviously primarily CO 5σ in character while the unoccupied $5\sigma^*$ orbital is mostly metal in character. The σ bond is usually referred to as the σ -donation portion of the CO-metal bond.² It is accompanied by a π bond formed from the metal d levels and the unoccupied gas-

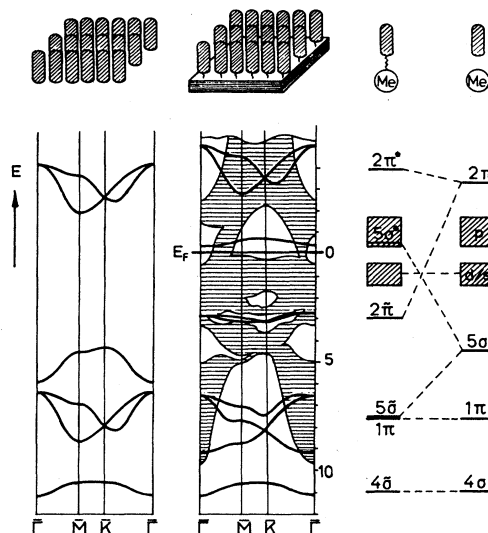


FIG. 1. One-electron scheme of a CO-metal interaction. Left-hand panel: band structure of an ordered CO array without CO-metal interaction. Center panel: band structure of an ordered CO overlayer with CO-metal interaction. Right-hand panel: molecular-orbital scheme of a CO-metal interaction.

phase CO 2π levels, forming the bonding $2\pi^*$'s and the antibonding unoccupied $2\pi^*$'s. The difference is that in this case the 2π orbitals are primarily metal in character, with a small admixture of the free CO 2π orbital. This is usually referred to as π backbonding.

The 5σ level of free CO is basically nonbonding in the molecule so the σ bond to the surface has little direct effect on the CO molecule. In contrast, the free CO 2π levels are antibonding with respect to the CO molecule so that the surface π bond weakens the CO bond for adsorbed CO. It is the characteristics of the 2π - d bonding that we shall address in this paper. But before the details of the experiment can be understood, it is important to appreciate the effect of the CO-CO interaction upon this picture of the energy levels of adsorbed CO.

The left-hand side of Fig. 1 shows what happens to the free CO levels when CO molecules are forced into a two-dimensional ordered array with the CO axis oriented in one direction. The CO levels now form two-dimensional bands dispersing as a function of the wave vector k_{\parallel} . The representation of this dispersion shown in Fig. 1 is calculated for a hexagonal structure using a simple tight-binding approach.^{3,4} As we shall show subsequently, a tight-binding scheme is sufficient to describe the energy levels of CO not involved in the bond to the surface, e.g., the 4σ level, because of the large CO-CO repulsive potential energy when the CO molecules approach each other either in the gas phase⁵ or on the surface.⁶

The center panel of Fig. 1 schematically shows what happens when an ordered layer of CO is brought into contact with a metal surface. In this figure the shaded portion of the energy versus parallel momentum represents the projection of the three-dimensional bulk bands of a metal-like Ni onto the two-dimensional surface. The 4σ band of adsorbed CO will be unaffected by the interaction with the substrate except for a shift to lower binding energy in a photoelectron spectrum due to the screening of the 4σ hole in the CO by the metal electrons.⁷ In principle the dispersion of the 5σ and the 1π bands of the adsorption system could also be described by the CO-CO interactions because neither orbital is changed dramatically as a consequence of the bonding.^{3,4} But the σ bonding will cause the 5σ energy level to shift downwards relative to the 1π , causing the two levels to be nearly degenerate.⁷ This allows the 5σ and 1σ bands to mix or hybridize forming hybridization gaps in the two-dimensional band structure^{1,3} as shown by the dashed lines in the center panel of Fig. 1. Since the unoccupied $2\pi^*$ levels are primarily CO 2π in character the dispersion of these levels seen in an inverse photoemission experiment^{8,9} should be similar to the dispersion calculated for an isolated CO layer.

It is appropriate to ask how well the experimental data and theoretical calculations agree with the picture presented above. All experiments and theory agree upon the qualitative nature of the downward shift of the 5σ band towards the 1π bands.⁷ The qualitative nature of the unoccupied $2\pi^*$'s seems to be confirmed by experimental measurements and simple theoretical calculations.⁸ Likewise, the detailed features of the two-dimensional dispersion of the CO-derived bands have

been successfully explained theoretically using a tight-binding scheme with the CO wave functions taken from a gas-phase calculation.⁸ Figure 2 shows the remarkable agreement between theory and experiment for the 4σ band in quite different adsorption systems. The left-hand curve displays the 4σ dispersion for the incommensurate $(2\sqrt{3} \times 2\sqrt{3})R 30^\circ$ ordered structure of CO adsorbed on Co(0001) (Ref. 3), whereas the right-hand curve shows the 4σ dispersion for the $(2 \times 1) p2mg$ structure of CO on Ni(110).

The unit cell of the latter structure contains two molecules and consequently two 4σ bands were found.⁴ The good agreement between experiment and theory seen for the 4σ bands is also present for the hybridized 5σ and 1π bands.⁴ The parts of the CO-bonding picture that are missing are the mostly metal levels, i.e., the $2\pi^*$'s and the $5\sigma^*$. There has been no report in literature of an observation of the unoccupied $5\sigma^*$ and the several observations of bands tentatively assigned to the $2\pi^*$ levels are all questionable, due to either the experimental data set or complexities of the technique.¹⁰⁻¹² We have taken advantage of the high CO density and unique symmetry of the $(2 \times 1) p2mg$ structure of CO on Ni(110) (Refs. 4, 13, and 14) to map out using angle-resolved photoemission the two-dimensional dispersion of the 2π bands (the π - d bands).

Low-energy electron diffraction (LEED) investigations of CO adsorption on the (110) faces of Ni (Refs. 14 and 15), Pd (Refs. 15 and 16), Pt (Ref. 15), Ir (Refs. 15 and 17), and Rh (Ref. 18) all show the presence of an ordered surface phase for one monolayer CO coverage. The LEED pattern is like a (2×1) , except that the fractional-order beams in the $[1\bar{1}0]$ azimuth are missing at all energies.¹⁵ The origin of this pattern was recognized by Lambert¹⁵ as resulting from a structure with two different CO molecules per unit cell, and he consequently labeled the symmetry as $p1g1$. It is difficult to decide from a LEED observation alone whether the surface symmetry is $p1g1$ or $p2mg$ because the existence of the mirror plane along $[1\bar{1}0]$ cannot be concluded from the

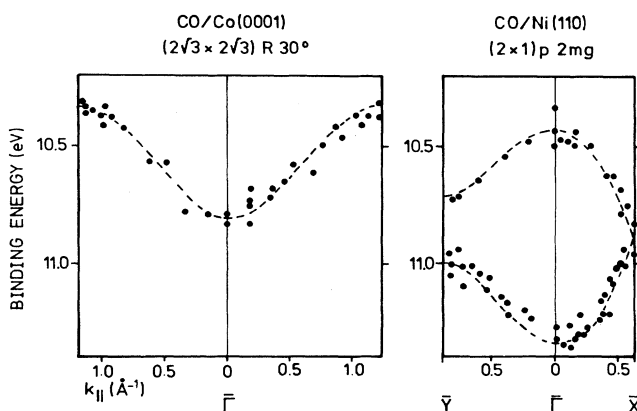


FIG. 2. Comparison of the calculated and the experimentally derived band dispersion of the 4σ bands for two different CO adsorption systems (Refs. 3 and 4).

LEED pattern. Both angle-resolved photoemission⁴ and electron-stimulated-desorption measurements¹⁹ show that the symmetry is *p2mg*, caused by the CO molecules being tilted strongly parallel to the [001] direction.

The best estimate at the present time of the structure of the (2×1) *p2mg* phase of CO on Ni(110) is shown in Fig. 3. As determined from LEED intensity analysis^{20,21} and high-resolution electron-energy-loss spectroscopy (HREELS) investigations^{22–25} the CO molecules occupy bridged positions along the rows of Ni atoms in the [110] direction. At coverages less than approximately 0.8 of a monolayer the molecules are bound in both the terminal and the bridge configuration standing upright on the surface. As the coverage is increased beyond 0.8 of a monolayer a transition occurs where the CO molecules are bound in a bent configuration as shown in Fig. 3. At saturation there is one CO molecule per Ni surface atom. To avoid the resulting strong lateral repulsion between adjacent molecules the two molecules in the unit cell tilt in opposite directions along the [001] azimuth.^{4,14,15,19} The tilt angle can, for instance, be determined by core-level x-ray photoelectron diffraction (XPD) (Refs. 26 and 27). When a photoelectron is emitted from the 1s core level of the carbon atom it will be diffracted by the oxygen atom of the molecule. This diffraction mechanism causes constructive interference of the original electron wave and the scattered wave along the axis of the CO

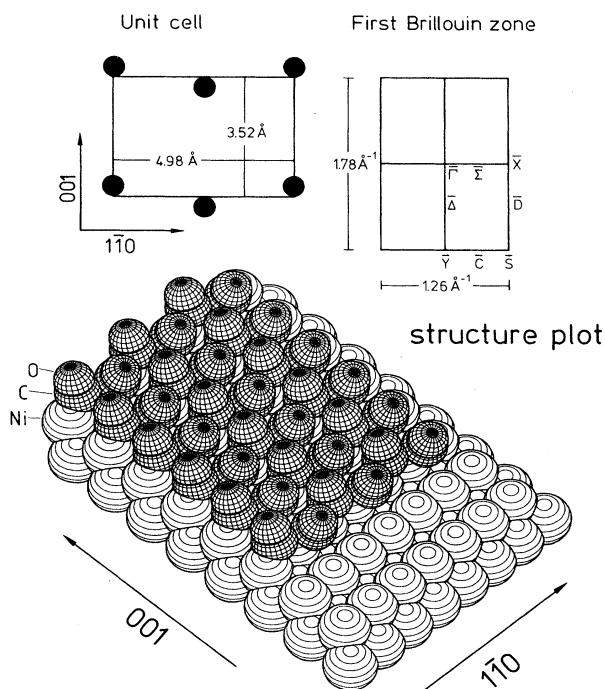


FIG. 3. Structure model of the adsorbate system Ni(110)/CO(2×1)-*p2mg*. Upper left-hand panel: size of the unit cell in real-space coordinates with the molecular positions schematically indicated. Upper right-hand panel: size, points, and lines of high symmetry within the unit cell. Lower panel: structure plot of the *p2mg* phase.

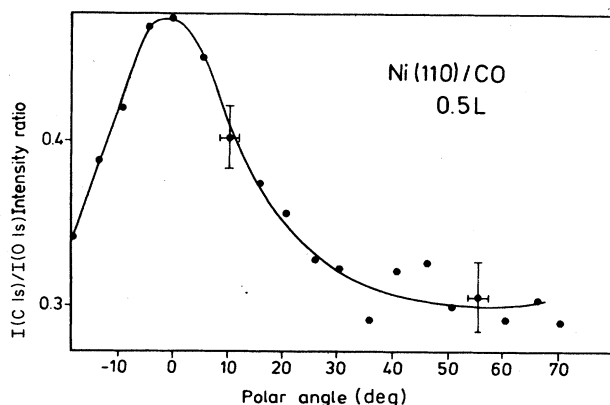


FIG. 4. Intensity of the C 1s emission normalized to the O 1s emission intensity as a function of the electron-emission angle along the [001] azimuth for a low CO coverage (0.5 L). The spectra were taken at a photon energy of $\hbar\omega = 1486.7$ eV.

molecule, resulting in a maximum of intensity along the molecular axis. Figures 4 and 5 show the intensity of the C 1s emission at different electron-excitation angles in the [001] azimuth for a low CO coverage and for the (2×1) *p2mg* structure.²⁶ The spectra were taken at a photon energy of $\hbar\omega = 1486.7$ eV. To eliminate polarization-dependent effects the C 1s emission has been normalized to the intensity of the O 1s emission. Figure 4 shows a clear maximum of the C 1s photoelectron intensity at normal incidence, indicating that the CO molecules axes are oriented perpendicular to the surface plane at low coverages. In contrast, the molecules in the (2×1) *p2mg* ordered phase are tilted by approximately 20°, giving rise to a maximum of intensity at this angle in Fig. 5. In good agreement with these findings, angle-resolved photoemission measurements indicate that the bent angle is $17^\circ \pm 2^\circ$ (Ref. 4), while electron-stimulated-desorption data favor a value of 18° .¹⁹

The combination of density of the layer and symmetry of this (2×1) *p2mg* phase of CO on Ni(110) is unique among CO adsorption systems. Table I lists the density and symmetry of several ordered phases of adsorbed CO. The least dense one is the physisorbed CO phase on

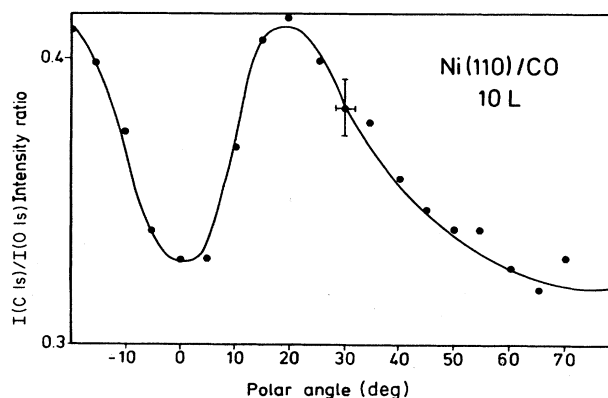


FIG. 5. Same as Fig. 4, but one monolayer of CO.

TABLE I. Density, symmetry, nearest-neighbor spacing, and 4σ bandwidth for several ordered phases of CO. Values marked by an asterisk are average nearest-neighbor spacings. The numbers in parentheses give the lower limit of the nearest-neighbor spacing, ignoring possible displacement and tilting effect.

Surface	Structure	Coverage	NN spacing (Å)	Density (Å ⁻²)	4σ dispersion (eV)	Ref.
Ag(111)	herringbone	$\frac{1}{3}$	5.00	0.040	<0.3	28
Os(0001)	$(\sqrt{3} \times \sqrt{3})R 30^\circ$	$\frac{1}{3}$	4.75	0.051		29
Ru(0001)	$(\sqrt{3} \times \sqrt{3})R 30^\circ$	$\frac{1}{3}$	4.69	0.052	0.09	30
Ir(111)	$(\sqrt{3} \times \sqrt{3})R 30^\circ$	$\frac{1}{3}$	4.69	0.052	0.2	31
Co(0001)	$(\sqrt{3} \times \sqrt{3})R 30^\circ$	$\frac{1}{3}$	4.34	0.061	0.15	3
Pd(111)	$c(4 \times 2)$	0.5	3.88	0.076	0.26	32
Ru(0001)	$(2\sqrt{3} \times 2\sqrt{3})R 30^\circ$	$\frac{7}{12}$	3.55*	0.092	0.5	30
Ir(111)	$(2\sqrt{3} \times 2\sqrt{3})R 30^\circ$	$\frac{7}{12}$	3.55*	0.092	0.4	31
Ni(100)	$c(2 \times 2)$	0.5	3.52	0.081	0.15	33
Fe(110)	$p(1 \times 2)$	0.5	3.41* (2.87)	0.086	0.3–0.4	34
Os(0001)	compression	0.68	3.32*	0.105	0.65	29
Co(0001)	$(2\sqrt{3} \times 2\sqrt{3})R 30^\circ$	$\frac{7}{12}$	3.29*	0.107	0.48	3
Ni(110)	$(2 \times 1) p2mg$	1.0	3.01* (2.49)	0.114	0.8	4

Ag(111) where the CO is lying down in a herringbone structure. The CO molecules are effectively much bigger when they are lying down so the density of molecules per Å² is only 0.04. The common $c(2 \times 2)$ structure of CO on Ni(100) (Ref. 33) has a nearest-neighbor spacing of 3.52 Å and a density of 0.081 molecules per Å². This nearest-neighbor separation should be compared to a repulsive barrier at a spacing of approximately 3 Å for gas-phase CO.⁵ In fact, the incommensurate Co(0001)/CO($2\sqrt{3} \times 2\sqrt{3}$) $R 30^\circ$ structure has a nearly-dense-packed configuration.³ In contrast to these ordinary CO-ordered layers, the Ni(110)/CO(2×1)- $p2mg$ structure has a higher density and a much shorter nearest-neighbor spacing. In the $[1\bar{1}0]$ direction the density is much too high for the CO molecules to exist on the surface in an upright configuration. They bent over to avoid the lateral stress.

The high density of this phase coupled with the unique symmetry made it possible to map out the two-dimensional dispersion of the adsorbate-induced 2π - d bands ($2\bar{\pi}$), using angle-resolved photoemission. The properties of these bands can be explained quite easily using a picture of overlayer and substrate wave functions which have been properly symmetry adapted. Using these wave functions it will be shown in the next section that the π - d bands can easily be described in terms of the Blyholder model for CO-substrate interaction.²

EXPERIMENT

The experiments were performed in two magnetically shielded ultrahigh-vacuum systems (VG, ADES400) containing facilities for LEED, Auger-electron spectroscopy, and residual-gas analysis with a quadrupole mass spectrometer. The analyzer is rotatable in two orthogonal planes and electrons are collected within an acceptance angle of $\pm 1.5^\circ$. The resolution in energy was typically 100 meV. Excitation of photoelectrons with polarized uv

light was achieved in one system by a capillary gas-discharge lamp, whereas the other system was attached to a toroidal-grating monochromator at the storage ring BESSY of the Berliner Elektronenspeicherring Gesellschaft für Synchrotronstrahlung mbH. The base pressure was in both systems below 10^{-8} Pa.

The Ni(110) crystal was spot-welded between two tungsten wires which were spot-welded to tungsten rods mounted on a sample manipulator. With liquid nitrogen the sample could be cooled down to 80 K. Heating was possible either directly or by electron impact onto the reverse side of the crystal. The crystal was cleaned by argon-ion bombardment, followed by annealing. Adsorption of CO during cool-down resulted in a well-ordered (2×1) $p2mg$ structure at liquid-nitrogen temperature.

SYMMETRY CONSIDERATIONS AND DISCUSSION

Figure 6 shows photoelectron spectra taken in normal emission with unpolarized radiation to show the features that will be discussed in this paper. Curve *a* is a spectrum of a clean Ni(110) surface showing the d bands within 1 eV of the Fermi energy. Curve *b* is from a saturation coverage of CO at room temperature where the coverage is below one monolayer and the adsorbate layer is not well ordered. This more conventional CO adsorption spectrum shows the CO $5\bar{\sigma}$ and $1\bar{\pi}$ levels in the range around 7 eV binding energy and the $4\bar{\sigma}$ level at 11 eV. Notice that there is a broad feature around 2 eV binding energy which has been shaded. Curve *c* of Fig. 6 is for the (2×1) $p2mg$ structure. Several features are appreciably different compared to the spectrum shown in curve *a*. First, the region of the CO $5\bar{\sigma}$ and $1\bar{\pi}$ energy levels is obviously more complicated, as is evident from the existence of a multitude of peaks. Also the region from 1 to 3 eV shows several well-pronounced features. It is this latter region that we will discuss in this paper. The dispersion of the CO-derived $5\bar{\sigma}$, $1\bar{\pi}$, and $4\bar{\sigma}$ bands

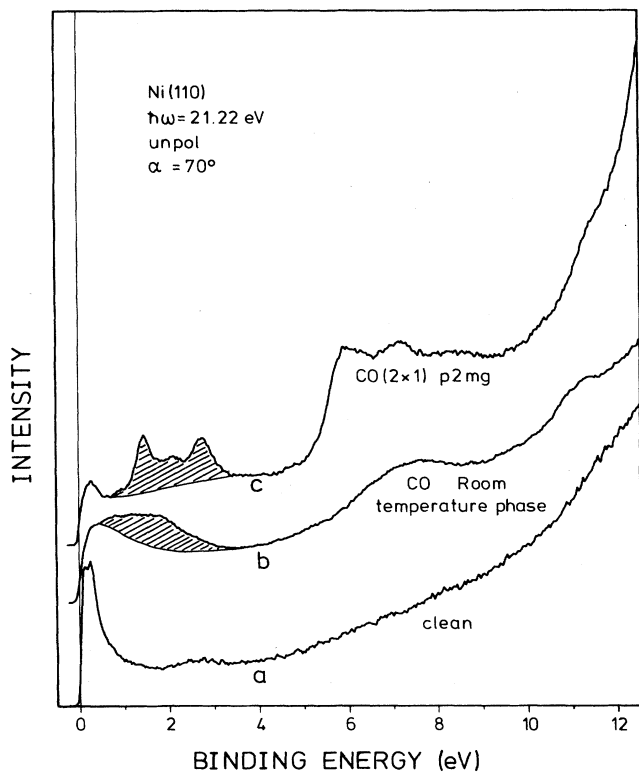


FIG. 6. Normal-emission photoelectron spectra of clean and adsorbate-covered Ni(110) taken with unpolarized light of a He resonance lamp.

has already been described.⁴ In this section we will show that the features in the photoemission spectra induced by the CO(2×1) p2mg structure in the Ni *d*-band region are due to two-dimensional states that are primarily Ni *d* in character, i.e., the CO 2 π -Ni *d* bands.

A set of normal-emission photoelectron spectra showing the development of the structures below the *d* bands as a function of CO coverage is displayed in Fig. 7. Two quite striking observations can be made in this figure. Firstly, notice how rapidly the *d* bands are attenuated with increasing CO coverage. The *d* bands are nearly completely removed at an exposure of 0.8 L CO and there is no dramatic further change when the (2×1) p2mg structure is formed. Secondly, one notices a dramatic increase of the intensity of the CO-induced peaks below the *d*-band region when the CO overlayer goes into the (2×1) p2mg phase [above 0.8 of a monolayer (Ref. 22)]. The increased intensity is not solely a consequence of the increased density, but more likely related to the unique symmetry and bonding configuration of this structure.

To discuss and analyze the experimental data, the symmetry of the two-dimensional adsorbate as well as the substrate surface wave functions have to be considered. We shall adopt the following procedure: since we are concerned with CO 2 π -Ni 3*d* interactions, we separately form symmetry-adapted CO 2 π overlayer wave functions and two-dimensional substrate wave functions. We clas-

sify them according to their symmetries and then consider possible interactions between the two subsets.

Figure 8 shows the two-dimensional overlayer 2 π wave functions at three symmetry points of the surface Brillouin zone (SBZ). The 2 π molecular orbitals are divided into two halves that are separated by a nodal point in the wave function. To visualize the phase factor of the wave functions which changes as a function of k_{\parallel} , either of these halves is half-shaded in Fig. 8. The angle of the shaded region with respect to the center of a specific part of a specific MO is equivalent to its phase. Due to the twofold symmetry of the system, the two components of the 2 π molecular orbital which are degenerate in the free molecule are split. We represent these two components throughout this study as π_x [Fig. 8(a)] and π_y [Fig. 8(b)] wave functions. In this paper the *X* direction is defined as the in-plane direction along the [110] azimuth and *Y* denotes the in-plane direction along the [001] azimuth. The situation depicted in Fig. 8 for the 2 π wave functions is identical to the one already discussed for the 1 π wave functions in Ref. 4. The main point is that the p2mg structure cannot be described by a primitive unit cell containing only one molecule per unit cell. As indicated in

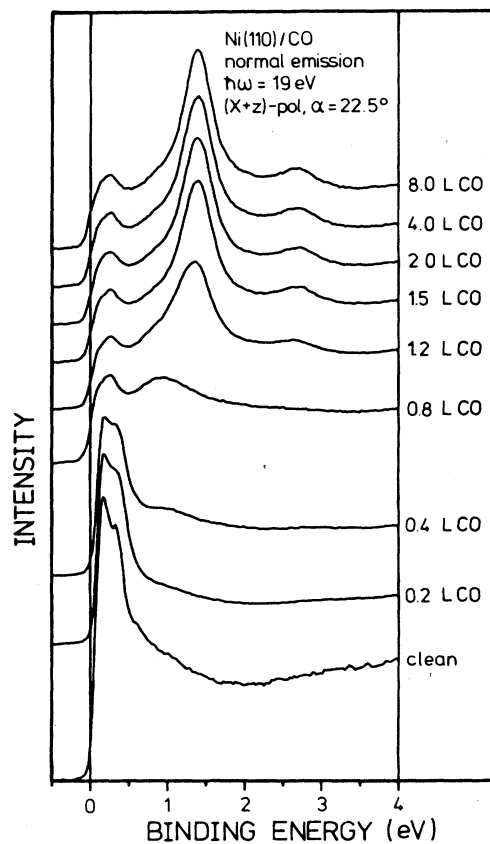


FIG. 7. Photoelectron spectra of Ni(110) in normal emission for different (CO) coverages, taken with primarily *X*-polarized synchrotron radiation of $\hbar\omega = 19$ eV. The notation (*X+z*) means *X*-polarized light with a little admixture of *Z*-polarized light.

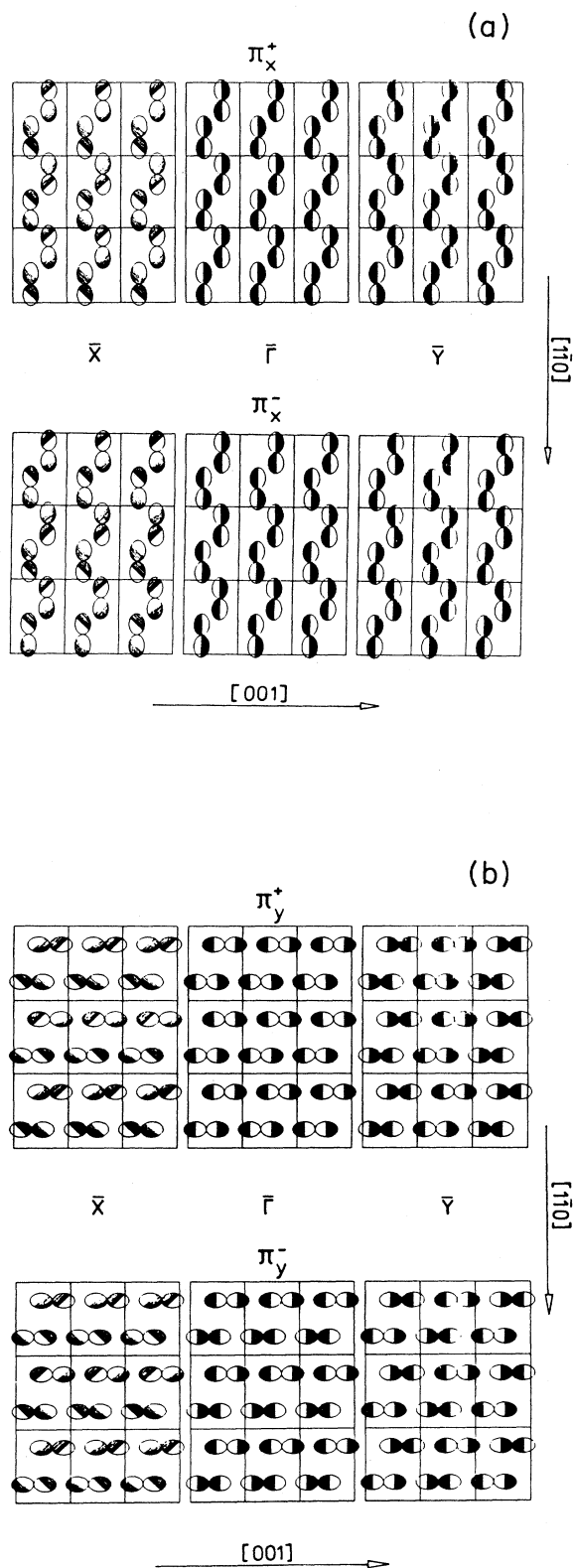


FIG. 8(a). Schematic real-space representation of the CO $2\pi_x$ -derived bands at three high-symmetry points of the (2×1) $p2mg$ SBZ. (b) Same as Fig. 8(a), but $2\pi_y$ -derived bands.

Fig. 3 and already discussed in Ref. 4, there are two molecules per unit cell. For a discussion of the symmetry of the bands, linear combinations of the molecular CO wave functions located at the positions of the two molecules have to be formed. Consequently, and in line with our previous analysis of the CO $4\sigma^-$, CO $5\sigma^-$, and CO 1π -derived band structure, the bonding and antibonding combinations of the π_x and π_y orbitals give rise to four bands at $\bar{\Gamma}$ labeled $2\pi_y^-$, $2\pi_y^+$, $2\pi_x^-$, and $2\pi_x^+$. The + and - signs refer to the phase factor within the unit cell. An in-phase combination of two 2π functions is antibonding and thus energetically destabilized on a binding-energy scale compared to a laterally noninteracting adsorbate. The out-of-phase combination of two 2π functions is bonding and thus energetically stabilized. Due to the different lateral interactions along $[001]$ and $[1\bar{1}0]$, the energy differences between the bonding and antibonding combinations differ for the $2\pi_y$ and the $2\pi_x$ bands. In Tables II and III we labeled the bands at different points and along different directions of the SBZ according to the irreducible representations of the $p2mg$ symmetry group using the nomenclature of Litvin.³⁵ We have shown the results for bridged and on-top molecular coordination.

If we follow the bands in k space along the symmetry line $\bar{\Gamma}$ to \bar{X} (i.e., the \bar{S} direction), the + and - combinations pairwise degenerate at \bar{X} . The left-hand sides of Fig. 8 allow us to analyze the situation. At \bar{X} the absolute phase difference of the molecular orbitals of adjacent CO molecules is zero along $[001]$ and 90° along $[1\bar{1}0]$ for both the symmetric and antisymmetric linear combination. So the lateral interaction which is determined by the interaction integral and thus by the phase difference of the wave functions is also the same, resulting in a degeneracy of the bands at \bar{X} . In fact, Hund showed in 1936 that for a $p2mg$ structure all bands have to be degenerate on the entire \bar{X} - \bar{S} line, i.e., the line perpendicular to the glide plane.³⁶ Clearly, the wave-function plots indicate that the energy positions of the bands at \bar{X} have to be intermediate between the energies at $\bar{\Gamma}$ since there is an increasing antibonding character for the bonding combination, whereas there is a loss in antibonding character for the antibonding combination.

At \bar{Y} , however, there is no symmetry argument for band degeneracies. The right-hand sides of Figs. 8(a) and 8(b) indicate the reason. The phase change in this case occurs, unlike in the former case perpendicular to the glide plane. The wave functions and thus the bands are not energetically degenerate since the spatial separation between sites of equal phase is larger for the - than for the + bands.

The next step on our way to understand the mixing between the unoccupied CO 2π levels and the occupied metal substrate levels is to form a basis of two-dimensional Ni bands from the occupied d and s electrons. Figures 9(a)–9(e) show schematic pictures of the wave functions at the same points, i.e., $\bar{\Gamma}$, \bar{X} , and \bar{Y} , that have been discussed above for the free-adsorbate layer. Due to the CO-Ni interaction the symmetry of the surface metal layer is not $p2mm$ as it would be in the clean Ni case, but $p2mg$. So the unit cell contains two Ni

TABLE II. Symmetry-selection rules for bridge-bonded CO.

Representation	CO 2π	Ni valence states	Polarization
Γ_1	$2\pi_y^-$	$s^+, d_{z^2}^+, d_{xy}^-, d_{x^2-y^2}^+$	Z
Γ_2	$2\pi_y^+$	d_{xz}^-, d_{yz}^+	Y
Γ_3	$2\pi_x^-$	$s^-, d_{z^2}^-, d_{xy}^+, d_{x^2-y^2}^-$	
Γ_4	$2\pi_x^+$	d_{xz}^+, d_{yz}^-	X
Σ_1	$2\pi_y^-, 2\pi_x^+$	$s^+, d_{z^2}^+, d_{xy}^-, d_{x^2-y^2}^+, d_{xz}^+, d_{yz}^-$	Z, X
Σ_2	$2\pi_y^+, 2\pi_x^-$	$s^-, d_{z^2}^-, d_{xy}^+, d_{x^2-y^2}^-, d_{xz}^-, d_{yz}^+$	Y
Δ_1	$2\pi_y^-, 2\pi_y^+$	$s^+, d_{z^2}^+, d_{xy}^-, d_{x^2-y^2}^+, d_{xz}^-, d_{yz}^+$	Z, Y
Δ_2	$2\pi_x^-, 2\pi_x^+$	$s^-, d_{z^2}^-, d_{xy}^+, d_{x^2-y^2}^-, d_{xz}^+, d_{yz}^-$	X

atoms and again we have to consider in-phase and out-of-phase combinations of the Ni valence orbital wave functions. By choosing this basis we can classify the pure Ni bands according to the global symmetry of the interacting overlayer, so that by pure symmetry arguments we can tell in the last step (see below) which of the substrate bands can couple to the CO overlayer bands.

Figure 9(a) shows schematic real-space representations of two-dimensional Ni bands formed from Ni d_{z^2} - s hybrid orbitals. As in the case of the CO 2π levels upon reaching the \bar{X} point, the bonding and antibonding combinations yield wave functions of identical energy. This means that there has to be a band degeneracy in the Ni d bands as well, dictated by symmetry. Again, towards \bar{Y} the degeneracy does not occur for the same reasons discussed for the CO 2π levels. Very similar analysis holds for the wave functions shown in Figs. 9(b)–9(e). In all cases the bands are forced to degenerate at \bar{X} , whereas they are split at $\bar{\Gamma}$ and \bar{Y} . Of course, the magnitude of the interaction depends on the orbital-specific Ni-Ni interactions. The classification of the bands according to the representations of the symmetry group *p2mg* is given in Table II for the position of the mirror plane between two Ni atoms and in Table III for the position of the mirror plane through the Ni atoms. Since only bands belonging to the same representation can interact, it is immediately clear from these tables which substrate level can couple to which CO 2π overlayer band. But it is also obvious that the result depends on the positions of the

mirror plane. Since for bridge-bonded CO the mirror plane goes through the CO molecules, Table II will be used throughout this paper, whereas Table III accounts for a possible on-top bonding site. Note, if a definitive assignment of the band character was possible from experiment, photoemission could be used to definitely assign the adsorption site in the present case.

We are now prepared to discuss the interaction between overlayer and substrate bands in more detail. Consider, for instance, the interaction of the CO $2\pi_y^+$ state with the Ni valence bands. From Table II it can be seen that at $\bar{\Gamma}$ the $2\pi_y^+$ band transforms according to Γ_2 . Thus it can interact with the Ni bands d_{xz}^- and d_{yz}^+ . The result will be three Γ_2 bands composed of the pure states $2\pi_y^+$, d_{xz}^- , and d_{yz}^+ . The band which is mostly $2\pi_y^+$ in character will be unoccupied and antibonding with respect to the Ni-CO interaction. From bremsstrahlung-isochromat-spectroscopy (BIS) experiments it is known that this band is located several eV above E_F .⁸ The remaining two bands are occupied and mostly metal in character. Energetically they are located in the range of the pure metal d bands. It should be noted that not only CO 2π and Ni valence bands interact, but also different Ni bands belonging to the same representation. Considering this the nomenclature that we shall use in the following for reasons of simplicity is not really correct. The assignment of a special band to be, for instance, “the $2\pi_y^+ - d_{yz}^+$ ” band just means that this band is mostly d_{yz}^+ in character with a usually small admixture of CO $2\pi_y^+$.

TABLE III. Symmetry-selection rules for terminal-bonded CO.

Representation	CO 2π	Ni valence states	Polarization
Γ_1	$2\pi_y^-$	$s^+, d_{z^2}^+, d_{x^2-y^2}^+, d_{yz}^-$	Z
Γ_2	$2\pi_y^+$	$s^-, d_{z^2}^-, d_{x^2-y^2}^-, d_{yz}^+$	Y
Γ_3	$2\pi_x^-$	d_{xz}^-, d_{xy}^+	
Γ_4	$2\pi_x^+$	d_{xz}^+, d_{xy}^-	X
Σ_1	$2\pi_y^-, 2\pi_x^+$	$s^+, d_{z^2}^+, d_{xy}^-, d_{x^2-y^2}^+, d_{xz}^+, d_{yz}^-$	Z, X
Σ_2	$2\pi_y^+, 2\pi_x^-$	$s^-, d_{z^2}^-, d_{xy}^+, d_{x^2-y^2}^-, d_{xz}^-, d_{yz}^+$	Y
Δ_1	$2\pi_y^-, 2\pi_y^+$	$s^+, s^-, d_{z^2}^+, d_{z^2}^-, d_{x^2-y^2}^+$ $d_{x^2-y^2}^-, d_{yz}^+, d_{yz}^-$	Z, Y
Δ_2	$2\pi_x^-, 2\pi_x^+$	$d_{xz}^+, d_{xz}^-, d_{xy}^+, d_{xy}^-$	X

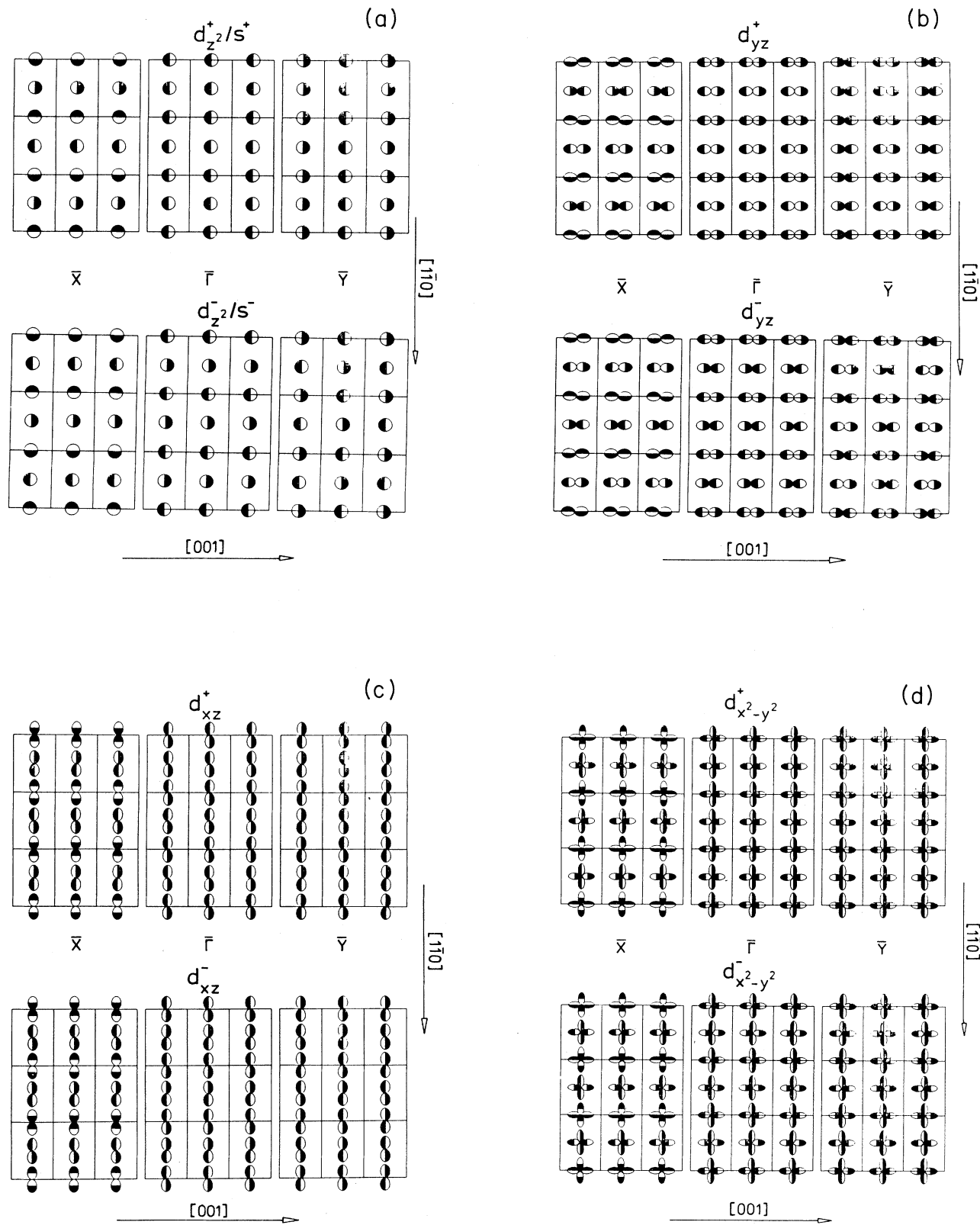


FIG. 9(a). Schematic real-space representation of the Ni d_{z^2-s} -derived bands at the surface of the adsorbate system Ni(110)/CO(2 \times 1)- $p2mg$ at three high-symmetry points of the SBZ. (b) Same as Fig. 9(a), but d_{yz} -derived bands. (c) Same as Fig. 9(a), but d_{xz} -derived bands. (d) Same as Fig. 9(a), but $d_{x^2-y^2}$ -derived bands. (e) Same as Fig. 9(a), but d_{xy} -derived bands.

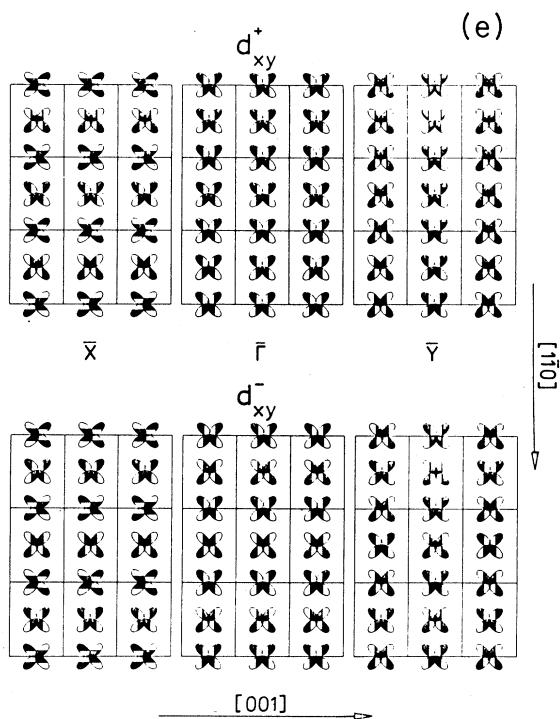


FIG. 9. (Continued).

The also existing but comparably small amount of d_{xz}^- admixture is neglected by this nomenclature.

It can also be seen from Table II that the composition of the bands is not constant but a function of the wave vector \mathbf{k}_{\parallel} . Along $\bar{\Sigma}$, for instance, the bands that belong to Γ_2 at $\bar{\Gamma}$ now transform according to Σ_2 , which allows for an interaction of all orbitals tabulated in the Σ_2 row of Table II. This means that the composition of a band at, for instance, \bar{X} may differ significantly from its composition at $\bar{\Gamma}$. The latter point gets important when we discuss the properties of the observed band structure of the π - d bands.

The Ni substrate bands that interact most strongly with the CO 2π bands are formed from the Ni d_{z^2-s} hybrids [Fig. 9(a)], the Ni d_{yz} [Fig. 9(b)], and the Ni d_{xz} orbitals [Fig. 9(c)] because they are directed towards the CO 2π molecular orbitals. The Ni $d_{x^2-y^2}$ and d_{xy} orbitals [Figs. 9(d) and 9(e)] are located within the surface plane and are expected to be not so important for the CO 2π -Ni interaction. Due to the spatial form of these orbitals, they will only show weak emission in normal excidence of the electrons. Thus the $d_{x^2-y^2}$ - and d_{xy} -derived hybrid bands will be neglected when discussing normal-emission spectra.

Figure 10 shows a set of photoelectron spectra for various collection angles in both the $\bar{\Sigma}$ [panel (a)] and the $\bar{\Delta}$ direction [panel (b)] of the $p2mg$ SBZ using X -polarized light of $\hbar\omega = 19$ eV. The vertical tic marks indicate the peak positions as a function of the wave vector \mathbf{k}_{\parallel} shown on the right of each panel. Due to the strong CO-Ni interaction the d -band emission of the clean Ni(110) surface

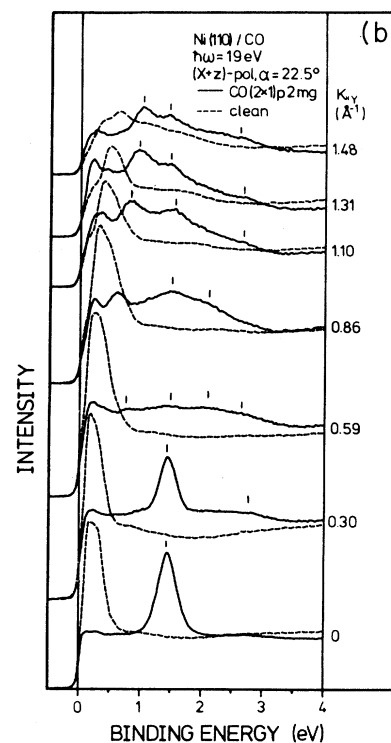
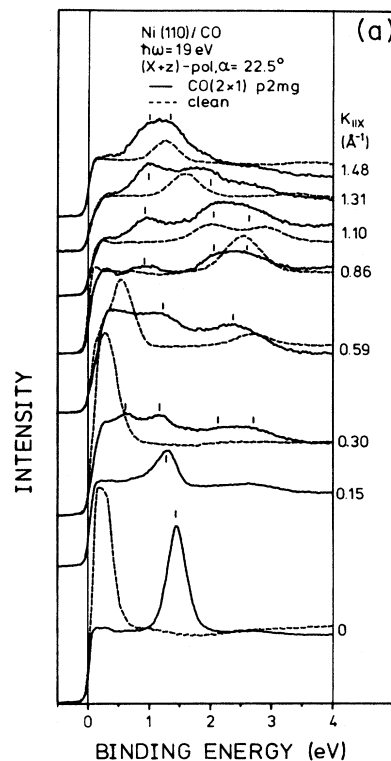


FIG. 10. (a) Series of photoelectron spectra of the valence-band region of Ni for clean (dashed) and CO-covered (solid) Ni(110) taken with primarily X -polarized light ($\hbar\omega = 19$ eV) as a function of the electron-excidence angle along the $[1\bar{1}0]$ direction. (b) Same as (a), but for the $[001]$ direction.

is almost completely removed upon CO adsorption and replaced by the emission of the π - d bands. Panel (a) shows the π - d bands at 2.0 and 2.7 eV binding-energy dispersing in a parallel fashion until at a wave vector $k_{\parallel} = 0.59 \text{ \AA}^{-1}$ which is near the \bar{X} point of the SBZ the two emissions coincide. Going to higher k_{\parallel} values the peaks start to separate again. This behavior is a consequence of the $p2mg$ symmetry of the overlayer, which allows only for the existence of twofold degenerate bands at \bar{X} .

After these remarks, we now discuss the properties of the observed band structure of the occupied π - d bands (Fig. 11). The solid lines show the band dispersion as observed by experiment ignoring possible hybridization gaps. The four experimental points at $\bar{\Gamma}$ in Fig. 11 are the π - d features shown in Fig. 12. The polarization dependence of these states as obtained from Fig. 12 can be used to identify the character of the bands at $\bar{\Gamma}$. The 2.7-eV state is excited by Z-polarized light only and thus it transforms according to Γ_1 . Neglecting the $d_{x^2-y^2}$ - and d_{xy} -derived bands, this feature can be identified from Table II to be the $2\pi_y^- - d_z^+ - s^+$ hybrid band. In this case the amount of s character in the wave function cannot be ignored since the d_z - s mixing is known to be strong.³⁷

In a similar fashion 2.0-eV feature can be assigned. This state belongs to the irreducible representation Γ_2 and thus has to be one of the hybrid bands $2\pi_y^+ - d_{yz}^+$ and $2\pi_y^+ - d_{xz}^-$. To further identify this band its dispersion as shown by the solid lines in Fig. 11 can be considered. If this band was mainly d_{xz} in character at $\bar{\Gamma}$, there should not be much dispersion along $\bar{\Delta}$ because the interaction of the d_{xz} -derived bands is only weak along [001]. Figure 10 shows that the dispersion bandwidth along $\bar{\Delta}$ is 0.75 eV, which is the greatest bandwidth of all observed π - d bands. From this we assign the main character of this band to be d_{yz} since the d_{yz} orbitals interact significantly along [001], giving rise to a much greater dispersion

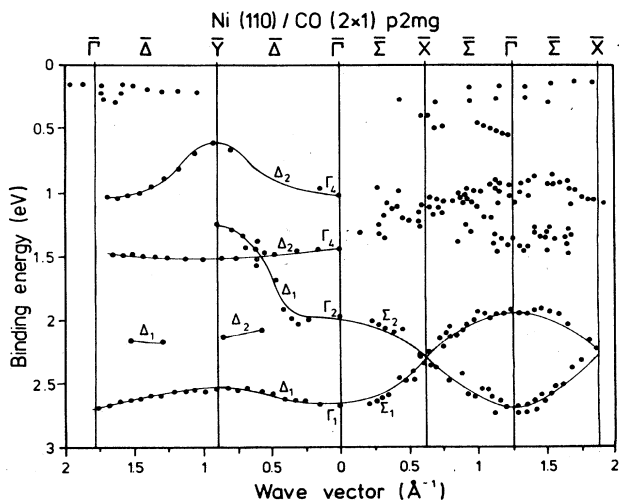


FIG. 11. Experimentally determined dispersions of the π - d bands along two high-symmetry directions of the SBZ.

bandwidth compared to the d_{xz} -derived bands. The remaining two π - d features at 1.0 and 1.5 eV in Fig. 12 are excited only by X-polarized light, indicating Γ_4 symmetry. According to Table II the metal part of their wave functions has to have d_{xz}^+ or d_{yz}^- character, respectively. An analysis like that done for the 2.0-eV feature shows that the main character of the 1.0-eV feature has to be d_{yz}^- , whereas the 1.5-eV feature has to be d_{xz}^+ in character.

There are two additional bands at a binding energy of approximately 2.2 eV around \bar{Y} , belonging to the irreducible representations Δ_1 and Δ_2 , respectively. Since the Δ_1 band dispersing from 2 eV at $\bar{\Gamma}$ to 1.25 eV at \bar{Y} in the first Brillouin zone will, of course, also exist in the second Brillouin zone, the two experimental data points making up the Δ_1 band in the second SBZ around 2.2 eV may belong to this band. The Δ_2 band near \bar{Y} at 2.2 eV must transform according to either Γ_3 or Γ_4 at $\bar{\Gamma}$. Table II shows that there are only two bands belonging to Γ_4 at $\bar{\Gamma}$. These are the two bands in the binding-energy range from 0.75 to 1.5 eV along $\bar{\Delta}$, and thus the Δ_2 band at 2.2 eV must belong to the representation Γ_3 at $\bar{\Gamma}$. The symmetry-selection rules in Table II show that such a state cannot be excited by either polarization of the light

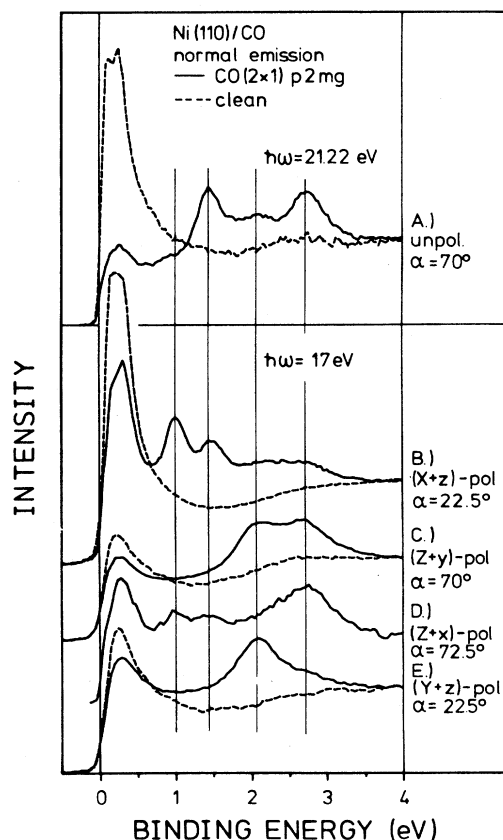


FIG. 12. Photoemission spectra of the valence-band region of Ni for clean (dashed) and CO-covered (solid) Ni(110) in normal emission. The three lower spectra were taken with different polarizations of the incident light.

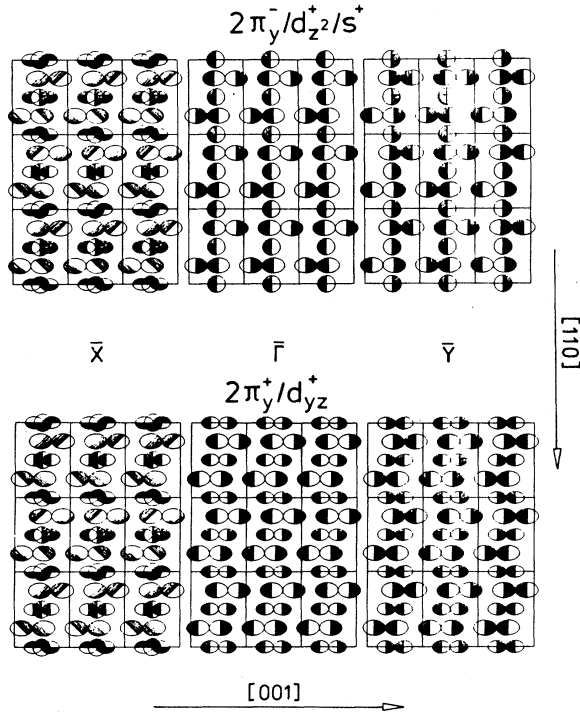


FIG. 13. Schematic real-space representation of the $2\pi_y^+$ - d_{yz}^+ - and the $2\pi_y^-$ - d_{yz}^+ -derived π - d bands at three different high-symmetry points of the SBZ.

and so this band could not be observed in the normal-emission spectra.

The experimental points within 0.5 eV below E_F could not be assigned along either direction. Because the main part of the substrate emission occurs in this energetic range, these features may be due to surface umklapp processes. However, emission from hybrid bands in this energy range cannot be conclusively excluded yet.

The range from 1.0 to 1.5 eV binding energy contains many data points along $\bar{\Sigma}$ that could not be assigned to definite bands. In normal emission ($\bar{\Gamma}$) in this range only the two Γ_4 features are observed. Since the symmetry allows only for twofold-degenerate bands at \bar{X} which have to belong to different representations along $\bar{\Sigma}$ and at $\bar{\Gamma}$, the two Γ_4 bands cannot degenerate at \bar{X} . Thus there must be two additional bands in this energetic range transforming according to either Γ_2 or Γ_3 at $\bar{\Gamma}$. The spectra show no additional emission in this range at $\bar{\Gamma}$ so that these bands will most probably belong to Γ_3 and thus will not be excitable in normal emission.

In contrast to the situation near the Fermi energy, the dispersion of the bands in the energetic range from 2 to 2.7 eV is rather clear. These bands degenerate at \bar{X} and their periodicity is just as demanded by the symmetry of the system. At \bar{X} certain symmetry operations transform each of the degenerate wave functions into the other one. The band starting at 2.0 eV from $\bar{\Gamma}$ was assigned to have $2\pi_y^-$ - d_{yz}^+ character at $\bar{\Gamma}$, whereas the band starting from 2.7 eV was assigned to have $2\pi_y^+$ - $d_{z^2}^+$ - s^+ character. The transformation of $2\pi_y^-$ into $2\pi_y^+$ is a symmetry operation

at \bar{X} , whereas the transformation of the metal part $d_{z^2}^+$ - s^+ into d_{yz}^+ and vice versa, of course, cannot be done by a symmetry operation. Thus the degeneracy of these bands apparently seems to not be possible by symmetry. But, as stated before, the composition of the bands is a function of the wave vector k_{\parallel} and thus the compositions of the bands at \bar{X} will differ from their composition at $\bar{\Gamma}$. To discuss this in more detail, assume, for instance, that the band starting at 2.0 eV from $\bar{\Gamma}$ ($2\pi_y^+$ - d_{yz}^+) begins to pick up $d_{z^2}^-$ - s^- character when dispersing along $\bar{\Sigma}$. This is possible since $2\pi_y^+$, d_{yz}^+ , and $d_{z^2}^-$ - s^- all belong to the same irreducible representation along $\bar{\Sigma}$. If the second band starts to pick up d_{yz}^- character, we get two bands at \bar{X} , the first one being composed of $2\pi_y^+$, d_{yz}^+ , and $d_{z^2}^-$ - s^- , and the second consisting of $2\pi_y^-$, d_{yz}^- , and $d_{z^2}^+$ - s^+ wave functions. These bands are allowed to degenerate at \bar{X} if they contain corresponding metal or CO wave functions of equal amounts. This means that if, for instance, the first band contains 10% d_{yz}^+ , the second one has to contain 10% d_{yz}^- . Figure 13 shows a plot of these bands at \bar{Y} , $\bar{\Gamma}$, and \bar{X} , assuming that the composition of the bands at \bar{Y} does not differ from their composition at $\bar{\Gamma}$. It should be noted that the qualitative composition of the bands as shown in Fig. 13 at \bar{X} and \bar{Y} is just an arbitrary choice. There is no specific physical reason to state that this must be the right composition although it may be the correct one.

As stated above, the bands in the range from 1.0 to 1.5 eV below E_F will most probably degenerate at \bar{X} with bands belonging to Γ_3 at $\bar{\Gamma}$. For these bands the same problems must be discussed; there must also be a change in the amount of the metal character of the wave functions along $\bar{\Sigma}$.

Figure 14 displays a set of normal-emission photoelectron spectra of the (2×1) p2mg phase of CO as a function of photon energy. Since the light was mostly X polarized, only the π - d states with Γ_4 symmetry are visible. As expected for true surface states these do not show any measurable dispersion at variation of k_{\perp} , but there is obviously a resonant enhancement of intensity at $\hbar\omega=16$ eV for the 1.0-eV state and at $\hbar\omega=19.5$ eV for the other one. This corresponds to kinetic energies of 15 and 18 eV, respectively.

Figure 15 shows the intensities of all four π - d features as a function of the kinetic energy of the emitted electrons. Two resonances are observable at 15 and 18 eV, respectively. We interpret these resonances to be due to unoccupied two-dimensional surface bands that are mostly metal in character. In particular, the strong resonance of the 1.5-eV feature can be interpreted analogously to a resonance observed for the d_{xz} -derived band of the Ni bulk band structure. Württemberg *et al.*³⁸ observed this resonance at a kinetic energy of 14 eV and interpreted it to be due to an excitation into an unoccupied band at the lower edge of the symmetry gap at the volume X point (Fig. 16). The character of this unoccupied band is not definitely known, but there exists a large cross section for an excitation of a d_{xz} -derived state into this unoccupied band. We may expect to find an unoccupied two-

dimensional band with the same character as the volume band at the surface too. Since the π - d state at 1.5 eV binding energy has been assigned to be mostly metal d_{xz} in character, we interpret its strong resonance at 18-eV kinetic energy to be due to an excitation into this unoccupied surface band. The latter one will, of course, be modified by the CO-Ni interaction with respect to the clean surface, giving rise to a shift of the kinetic energy from 14 eV in the case of the bulk band to 18 eV at the surface. For the second resonance of the π - d states at 15 eV, no corresponding resonance of the bulk bands is known. But due to the $p2mg$ symmetry at the surface, out-of-phase combinations of unoccupied metallic orbitals have to be additionally taken into account. Such bands can exist at the surface only and one of them may give rise to the resonance of intensity at 15-eV kinetic energy.

One may argue that the features that we assigned to be π - d states could result from a diffraction of the outgoing electrons by the CO superstructure, i.e., they could be due to surface umklapp processes. This can be ruled out by measuring the position of the peaks as a function of photon energy for a fixed value of k_{\parallel} . If the states are truly two dimensional in character, there will be no dispersion with photon energy.⁷ Figure 14 shows a set

of normal-emission energy distributions for X -polarized light as a function of photon energy. Figure 12 showed that the 1.0- and 1.5-eV peaks were excited by X -polarized light. Both of these peaks can be seen in the spectra over a wide photon-energy range without any measurable dispersion. This proves that the assigned features of the (2×1) $p2mg$ phase originate from two-dimensional energy bands at the surface.

Finally, we would like to comment on a controversially discussed issue. Mainly, two theoretical models for the bonding of CO to transition metals are available from the literature, namely the Blyholder model² and the Anderson-Newns model.⁴⁰ It is the Blyholder model that we applied throughout this paper. It is described in the Introduction and visualized in Fig. 1. If we try to interpret our data in terms of the Anderson-Newns model we run into severe problems. This picture predicts the electronic CO-substrate interaction to result in a broad 2π resonance, centered some eV above the Fermi energy. The full width at half maximum (FWHM) of this feature should be several eV, leading to a tail extending below the Fermi level and thus to a certain degree of occupancy. It is this tail that should be detectable by photoemission. But the features that we get as the result of CO adsorption in the d -band regime cannot be interpreted as the

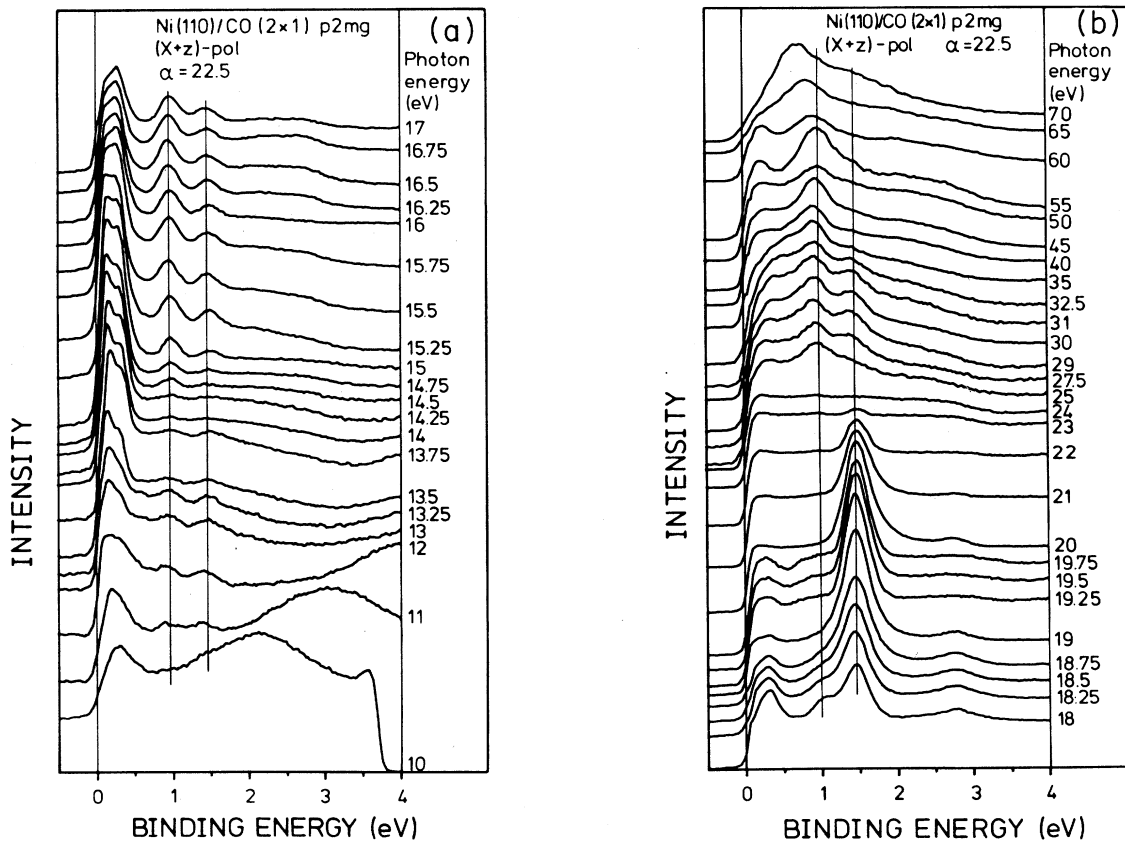


FIG. 14(a). Series of normal-emission photoelectron spectra of the Ni(110)/CO(2 \times 1)- $p2mg$ adsorbate system taken with primarily X -polarized light as a function of the photon energy. (b) Continuation of Fig. 14(a).

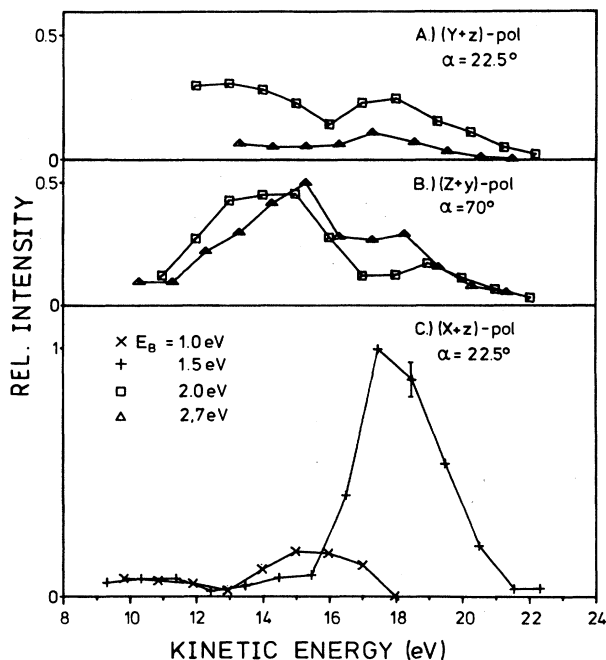


FIG. 15. Intensity of the π - d band emissions as a function of the kinetic energy of the emitted photoelectrons at normal incidence.

emission of the occupied tail of a broad, mostly unoccupied electronic state since they do not show the form of such a tail, i.e., they do not seem to extend above the Fermi level. Besides this, we find four states with different symmetries instead of one state. BIS measurements on the (2×1) $p2mg$ phase of CO on Ni(110) (Ref. 8) are also in contradiction with the predictions of the Anderson-Newns model since the $2\pi^*$ features found in the spectra do not extend below the Fermi level and the spectra also show more than one electronic state. In contrast to this, the application of the Blyholder model to either BIS and ultraviolet-photoemission-spectroscopy (UPS) results is possible without problems, leading to the conclusion that this model is much easier to use for the description of the CO-substrate interaction. This holds true at least in the case of the (2×1) $p2mg$ phase of CO adsorbed on Ni(110).

SUMMARY

In the present study we have presented results of polarization-dependent angle-resolved x-ray-photoemission-spectroscopy (ARUPS) measurements on the π - d backbonding bands of the adsorbate system Ni(110)/CO(2×1)- $p2mg$. These bands are located in the Ni valence-band regime at the surface of the substrate and result from the interaction of the CO 2π bands with the Ni $3d$ bands. Due to this interaction, the symmetry of the Ni surface layer is lowered from $p2mm$ to $p2mg$ and, as in the case of the molecular orbitals of the adsorbed CO molecules,⁴ instead of the pure Ni wave functions, symmetric and antisymmetric linear combinations

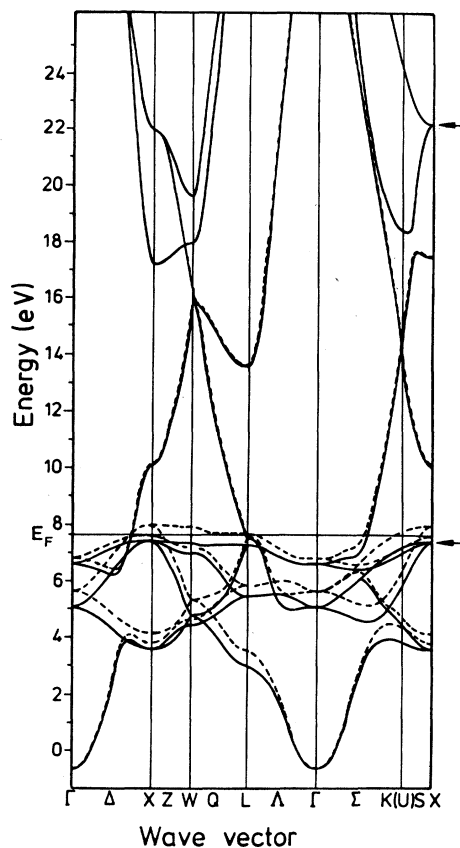


FIG. 16. Calculated Ni bulk band structure (Ref. 39). The initial and the final state of the intense transition at the X point of the bulk Brillouin zone are marked by arrows.

of these have to be considered. The π - d bands can then be described as linear combinations of the symmetry-adapted CO 2π and Ni $3d$ wave functions. Using the dipole-selection rules of the $p2mg$ space group and the experimentally determined band dispersions, a qualitative assignment of the character of the bands to definite linear combinations of Ni $3d$ and CO 2π bands can be derived. Since the π - d bands consist mostly of metal wave functions, they behave to a certain extent like the pure Ni bands and so for the d_{xz} -derived π - d surface band an intensity resonance was observed similar to a resonance found for the d_{xz} -derived band of bulk Ni.³⁸ Finally, we note that all properties of the π - d bands can easily be described in terms of the Blyholder model for the interaction of CO with transition-metal surfaces.²

ACKNOWLEDGMENTS

This work has been funded by the German Federal Minister for Research and Technology [Bundesminister für Forschung und Technologie (BMFT)] under Contract No. 05-327-AAB3. E.W.P. thanks the Alexander von Humboldt Foundation for financial support and H.-J.F. gratefully acknowledges financial support from the Fond der Chemischen Industrie.

- *Present address: Lehrstuhl für Physikalische Chemie I, Ruhr-Universität Bochum, D-4630 Bochum 1, Federal Republic of Germany.
- ¹H. Kühlenbeck, H. B. Saalfeld, M. Neumann, H.-J. Freund, and E. W. Plummer, *Appl. Phys A* **44**, 83 (1987).
- ²G. Blyholder, *J. Chem. Phys.* **68**, 2772 (1964); *J. Vac. Sci. Technol.* **11**, 865 (1974).
- ³F. Greuter, D. Heskett, E. W. Plummer, and H.-J. Freund, *Phys. Rev. B* **27**, 7117 (1983).
- ⁴H. Kühlenbeck, M. Neumann, and H.-J. Freund, *Surf. Sci.* **173**, 194 (1986).
- ⁵E. A. Mason and W. E. Rice, *J. Chem. Phys.* **22**, 843 (1964).
- ⁶J. C. Tracy and P. W. Palmberg, *J. Chem. Phys.* **51**, 4852 (1969).
- ⁷E. W. Plummer and W. Eberhardt, *Adv. Chem. Phys.* **49**, 533 (1982).
- ⁸H.-J. Freund, J. Rogozik, V. Dose, and M. Neumann, *Surf. Sci.* **175**, 651 (1986).
- ⁹F. J. Himpsel and Th. Fauster, *Phys. Rev. Lett.* **49**, 1583 (1982); Th. Fauster and F. J. Himpsel, *Phys. Rev. B* **27**, 1390 (1983); J. Rogozik, H. Scheidt, V. Dose, K. C. Prince, and A. M. Bradshaw, *Surf. Sci.* **145**, L481 (1984); J. Rogozik, V. Dose, K. C. Prince, A. M. Bradshaw, P. S. Bagus, K. Hermann, and Ph. Avouris, *Phys. Rev. B* **32**, 4296 (1985); P. D. Johnson, D. A. Wesner, J. W. Davenport, and N. V. Smith, *ibid.* **30**, 4860 (1984); J. Rogozik, J. Küppers, and V. Dose, *Surf. Sci.* **148**, L653 (1985).
- ¹⁰R. J. Smith, J. Anderson, and G. J. Lapeyre, *Phys. Rev. B* **22**, 632 (1980).
- ¹¹F. Boszo, J. Arias, J. T. Yates, R. M. Martin, and H. Metiu, *Chem. Phys. Lett.* **94**, 243 (1983).
- ¹²C. F. McConville, C. Somerton, and D. P. Woodruff, *Surf. Sci.* **139**, 75 (1984).
- ¹³H. H. Madden, J. Küppers, and G. Ertl, *J. Chem. Phys.* **58**, 3401 (1973); H. H. Madden and G. Ertl, *Surf. Sci.* **35**, 211 (1973).
- ¹⁴R. J. Behm, G. Ertl, and V. Penka, *Surf. Sci.* **160**, 367 (1985).
- ¹⁵R. M. Lambert, *Surf. Sci.* **49**, 325 (1975).
- ¹⁶H. Conrad, G. Ertl, J. Koch, and E. E. Latta, *Surf. Sci.* **43**, 462 (1974).
- ¹⁷K. Christmann and G. Ertl, *Z. Naturforsch* **28a**, 1144 (1973).
- ¹⁸R. A. Marbrow and R. M. Lambert, *Surf. Sci.* **67**, 489 (1977).
- ¹⁹W. Riedl and D. Menzel, *Surf. Sci.* **163**, 39 (1985).
- ²⁰D. J. Hannaman and M. A. Passler, *Surf. Sci.* **203**, 449 (1988).
- ²¹H. Davis and K. Müller (private communication).
- ²²B. A. Guernsey and W. Ho, *J. Vac. Sci. Technol. A* **3**, 1541 (1985).
- ²³J. C. Bertolini and B. Tardy, *Surf. Sci.* **102**, 131 (1981).
- ²⁴M. Nishijima, S. Masuda, Y. Sakisaka, and M. Onchi, *Surf. Sci.* **107**, 31 (1981).
- ²⁵P. R. Mahaffy and M. J. Dignam, *Surf. Sci.* **97**, 377 (1980).
- ²⁶U. Buskotte, Diplomarbeit, Universität Osnabrück, 1987.
- ²⁷D. A. Wesner, F. P. Coenen, and H. P. Bonzel, *Phys. Rev. Lett.* **60**, 11 (1988).
- ²⁸D. Schmeisser, F. Greuter, W. Plummer, and H.-J. Freund, *Phys. Rev. Lett.* **54**, 2095 (1985).
- ²⁹H. Kühlenbeck, H. B. Saalfeld, H.-J. Freund, and M. Neumann (unpublished).
- ³⁰P. Hofmann, J. Gossler, A. Zartner, M. Glanz, and R. D. Schnell, *Surf. Sci.* **161**, 303 (1985); D. Heskett, E. W. Plummer, R. A. de Paola, W. Eberhardt, and F. M. Hoffmann, *ibid.* **164**, 490 (1985).
- ³¹C. W. Seabury, E. S. Jensen, and T. N. Rhodin, *Solid State Commun.* **37**, 383 (1981).
- ³²R. Miranda, K. Wandelt, D. Rieger, and R. D. Schnell, *Surf. Sci.* **139**, 430 (1984).
- ³³K. Horn, A. M. Bradshaw, and K. Jacobi, *Surf. Sci.* **72**, 719 (1978).
- ³⁴E. S. Jensen and T. N. Rhodin, *Phys. Rev. B* **27**, 3338 (1983).
- ³⁵D. B. Litvin, *Thin Solid Films* **106**, 203 (1983).
- ³⁶F. Hund, *Z. Phys.* **99**, 119 (1936).
- ³⁷L. Salem and C. Leforestier, *Surf. Sci.* **82**, 390 (1979).
- ³⁸J. Württemberg, U. Herwig, E. Dietz, U. Gerhard, and H. Kühlenbeck, BESSY Annual Report, Berlin, 1985 (unpublished).
- ³⁹E. Marschall and H. Bross, *Phys. Status Solidi B* **90**, 241 (1978).
- ⁴⁰D. M. Newns, *Prog. Surf. Sci.* **9**, 1 (1978); B. Gumhalter, K. Wandelt, and Ph. Avouris, *Phys. Rev. B* **37**, 8048 (1988).